Asian Journal of Chemistry; Vol. 27, No. 9 (2015), 3285-3288

ASIAN JOURNAL OF CHEMISTRY

http://dx.doi.org/10.14233/ajchem.2015.18568

Microwave-Assisted Sol-Gel Preparation of $KY(WO_4)_2$:Ho^{3+}/Yb^{3+} Yellow Phosphors and Their Upconversion Photoluminescence Properties

CHANG SUNG LIM

Department of Advanced Materials Science and Engineering, Hanseo University, Seosan 356-706, Republic of Korea

Corresponding author: Tel/Fax: +82 41 6601445; E-mail: cslim@hanseo.ac.kr

Received: 7 August 2014; *Accepted*: 20 November 2014; *Published online*: 26 May 2015; AJC-17241

Double tungstate $KY_{1-x}(WO_4)_2$:Ho^{3+}/Yb^{3+} yellow phosphors with doping concentrations of Ho^{3+} and Yb^{3+} (x = Ho^{3+} + Yb^{3+}, Ho^{3+} = 0.05, 0.1, 0.2 and Yb^{3+} = 0.2, 0.45) were successfully prepared by the microwave-assisted sol-gel method and their upconversion photoluminescence properties was investigated. Well-crystallized particles, formed after heat-treatment at 900 °C for 16 h, showed a fine and homogeneous morphology with particle sizes of 2-5 μm. Under excitation at 980 nm, the upconversion intensity of $KY_{0.5}(MoO_4)_4$:$Ho_{0.05}Yb_{0.45}$ phosphor exhibited yellow emissions based on a strong 550 nm emission band in the green region and a strong 655 nm emission band in the red region. The Raman spectra of the particles indicated the presence of strong peaks at higher frequencies and a weak peak at lower frequency induced by the disorder of the $[WO_4]^{2-}$ groups with the incorporation of the Ho^{3+} and Yb^{3+} elements into the crystal lattice or by a new phase formation.

Keywords: Microwave, Sol-gel, Double tungstate, Yellow phosphors, Raman Spectroscopy.

INTRODUCTION

The lanthanide doped phosphors for upconversion (UC) luminescence have attracted so much attention due to the wide applications including lightening, flat panel display, photovoltaic and nano-biotechnology such as bio labeling and bio imaging[1-3]. The double tungstates possess the tetragonal Scheelite structure with the space group $I4_{1/a}$ and belong to the family of double tungstates compounds. It is possible for the trivalent rare earth ions in the disordered tetragonal-phase to be partially substituted by Ho^{3+} and Yb^{3+} ions, these ions are effectively doped into the crystal lattices of the tetragonal phase due to the similar radii of the trivalent rare earth ions (Re^{3+}). This results in high red emitting efficiency and superior thermal and chemical stability. In these compounds, W^{6+} is coordinated by four O^{2-} at a tetrahedral site, which makes $[WO_4]^{2-}$ relatively stable. Re^{3+} and M^{+} are randomly distributed over the same cationic sublattice and they are coordinated by eight O^{2-} from near four $[WO_4]^{2-}$ with a symmetry S_4 without an inversion center[4-6]. The $[WO_4]^{2-}$ group has strong absorption in the near ultraviolet region, so that energy transfers process from $[WO_4]^{2-}$ group to rare earth ions can easily occur, which can greatly enhance the external quantum efficiency of rare earth ions doped materials.

Many lanthanides such as Er^{3+}, Tm and Ho^{3+} are used as luminescent centers because of their abundant electronic energy levels are very convenient for realizing the conversion of near infrared light to visible light. Among the lanthanides ions, the Ho^{3+} ion as an activator is a promising upconversion luminescence center because of its unique luminescence in visible range, while the sensitizer enhances the upconversion luminescence efficiency. The Yb^{3+} ion is generally co-doped as a sensitizer owing to its strong absorption around 980 nm and can enhance the upconversion luminescence through energy transfer. Especially, the co-doped Yb^{3+} ion and Ho^{3+} ion can remarkably enhance the upconversion efficiency for the shift from infrared to visible light due to the efficiency of the energy transfer from Yb^{3+} to Ho^{3+} [7-9].

The lanthanides doped double tungsates have been prepared by the several processes. Compared with the usual methods, microwave synthesis has the advantages of a very short reaction time, small-size particles, narrow particle size distribution and high purity of final polycrystalline samples. Microwave heating is delivered to the material surface by radiant and/or convection heating, which is transferred to the bulk of the material *via* conduction[10]. A microwave-assisted sol-gel process is a cost-effective method that provides high homogeneity and is easy to scale-up and it is emerging as a viable alternative approach for the quick synthesis of high-quality luminescent materials. However, the synthesis of $KY(WO_4)_2$:Ho^{3+}/Yb^{3} phosphors by the microwave-assisted sol-gel method has not been reported.

In this study, $KY_{1-x}(WO_4)_4$:Ho^{3+}/Yb^{3+} phosphors with doping concentrations of Ho^{3+} and Yb^{3+} (x = Ho^{3+} + Yb^{3+}, Ho^{3+} = 0.05, 0.1, 0.2 and Yb^{3+} = 0.2, 0.45) phosphors were prepared by the cyclic microwave-assisted sol-gel method followed by heat treatment. The synthesized particles were characterized by X-ray diffraction (XRD), scanning electron microscopy (SEM) and energy-dispersive X-ray spectroscopy (EDS). The optical properties were examined comparatively using photoluminescence (PL) emission and Raman spectroscopy.

EXPERIMENTAL

Stoichiometric amounts of KNO_3 (99 %, Sigma-Aldrich, USA), $Y(NO_3)_3·6H_2O$ (99 %, Sigma-Aldrich, USA), $(NH_4)_6W_{12}O_{39}·xH_2O$ (99 %, Alfa Aesar, USA), $Ho(NO_3)_3·5H_2O$ (99.9 %, Sigma-Aldrich, USA), $Yb(NO_3)_3·5H_2O$ (99.9 %, Sigma-Aldrich, USA), citric acid (99.5 %, Daejung Chemicals, Korea), NH_4OH (A.R.), ethylene glycol (A.R.) and distilled water were used to prepare $KY(WO_4)_2$, $KY_{0.8}(WO_4)_2$:$Ho_{0.2}$, $KY_{0.7}(WO_4)_2$:$Ho_{0.1}Yb_{0.2}$ and $KY_{0.5}(WO_4)_2$:$Ho_{0.05}Yb_{0.45}$ compounds with doping concentrations of Ho^{3+} and Yb^{3+} (Ho^{3+} = 0.05, 0.1, 0.2 and Yb^{3+} = 0.2, 0.45). To prepare $KY(WO_4)_2$, 0.4 mol % KNO_3 and 0.067 mol % $(NH_4)_6W_{12}O_{39}·xH_2O$ were dissolved in 20 mL of ethylene glycol and 80 mL of 5M NH_4OH under vigorous stirring and heating. Subsequently, 0.4 mol % $Y(NO_3)_3·6H_2O$ and citric acid (with a molar ratio of citric acid to total metal ions of 2:1) were dissolved in 100 mL of distilled water under vigorous stirring and heating. Then, the solutions were mixed together under vigorous stirring and heating at 80-100 °C. At the end, highly transparent solutions were obtained and adjusted to pH = 7-8 by the addition of NH_4OH or citric acid. In order to prepare $KY_{0.8}(WO_4)_2$:$Ho_{0.2}$, the mixture of 0.32 mol % $Y(NO_3)_3·6H_2O$ with 0.08 mol % $Ho(NO_3)_3·5H_2O$ was used for the rare earth solution. In order to prepare $KY_{0.7}(WO_4)_2$:$Ho_{0.1}Yb_{0.2}$, the mixture of 0.28 mol % $Y(NO_3)_3·6H_2O$ with 0.04 mol % $Ho(NO_3)_3·5H_2O$ and 0.08 mol % $Yb(NO_3)_3·5H_2O$ was used for the rare earth solution. In order to prepare $KY_{0.5}(WO_4)_2$:$Ho_{0.05}Yb_{0.45}$, the rare earth containing solution was generated using 0.2 mol % $Y(NO_3)_3·6H_2O$ with 0.02 mol % $Ho(NO_3)_3·5H_2O$ and 0.18 mol % $Yb(NO_3)_3·5H_2O$.

The transparent solutions were placed into a microwave oven operating at a frequency of 2.45 GHz with a maximum output-power of 1250 W for 0.5 h. The working cycle of the microwave reaction was controlled very precisely using a regime of 40 s on and 20 s off for 15 min, followed by further treatment of 30 s on and 30 s off for 15 min. The ethylene glycol was evaporated slowly at its boiling point. Ethylene glycol is a polar solvent at its boiling point of 197 °C, this solvent is a good candidate for the microwave process. If ethylene glycol is used as the solvent, the reactions proceed at the boiling point temperature. When microwave radiation is supplied to the ethylene-glycol-based solution, the components dissolved in the ethylene glycol can couple. The charged particles vibrate in the electric field interdependently when a large amount of microwave radiation is supplied to the ethylene glycol. The samples were treated with ultrasonic radiation for 10 min to produce a light yellow transparent sol. After this, the light yellow transparent sols were dried at 120 °C in a dry oven to obtain black dried gels. The black dried gels were grinded and heat-treated at 900 °C for 16 h with 100 °C intervals between 600-900 °C. Finally, white particles were obtained for $KY(MoO_4)_2$ and pink particles for the doped compositions.

The phase composition of the synthesized particles was identified using XRD (D/MAX 2200, Rigaku, Japan). The microstructure and surface morphology of the $KY(MoO_4)_2$, $KY_{0.8}(WO_4)_2$:$Ho_{0.2}$, $KY_{0.7}(WO_4)_2$:$Ho_{0.1}Yb_{0.2}$ and $KY_{0.5}(WO_4)_2$:$Ho_{0.05}Yb_{0.45}$ particles were observed using SEM/EDS (JSM-5600, JEOL, Japan). The photoluminescence spectra were recorded using a spectrophotometer (Perkin Elmer LS55, UK) at room temperature. Raman spectroscopy measurements were performed using a LabRam Aramis (Horiba Jobin-Yvon, France). The 514.5 nm line of an Ar ion laser was used as the excitation source and the power on the samples was kept at 0.5 mW.

RESULTS AND DISCUSSION

Fig. 1 shows the X-ray diffraction patterns of (a) JCPDS 45-0472 data of $KY(WO_4)_2$, the synthesized (b) $KY(WO_4)_2$, (c) $KY_{0.8}(WO_4)_2$:$Ho_{0.2}$, (d) $KY_{0.7}(WO_4)_2$:$Ho_{0.1}Yb_{0.2}$ and (e) $KY_{0.5}(WO_4)_2$:$Ho_{0.05}Yb_{0.45}$ particles. All of the XRD peaks could be assigned to the monoclinic-phase $KY(WO_4)_2$, which was in good agreement with the crystallographic data of $KGd(MoO_4)_2$ (JCPDS 45-0472). This means that the obtained samples possess a monoclinic-phase after partial substitution of Y^{3+} by Ho^{3+} and Yb^{3+} ions and the ions are effectively doped into crystal lattices of the $KY(WO_4)_2$ phase due to the similar radii of Y^{3+} and by Ho^{3+} and Yb^{3+}. Post heat-treatment plays an important role in a well-defined crystallized morphology. To achieve a well-defined crystalline morphology, $KY(WO_4)_2$, $KY_{0.8}(WO_4)_2$:$Ho_{0.2}$, $KY_{0.7}(WO_4)_2$:$Ho_{0.1}Yb_{0.2}$ and $KY_{0.5}(WO_4)_2$:$Ho_{0.05}Yb_{0.45}$ phases need to be heat treated at 900 °C for 16 h. It is assumed that the doping amount of Ho^{3+}/Yb^{3+} has a great effect on the crystalline cell volume of the $KY(WO_4)_2$, because of the different ionic sizes and energy band gaps.

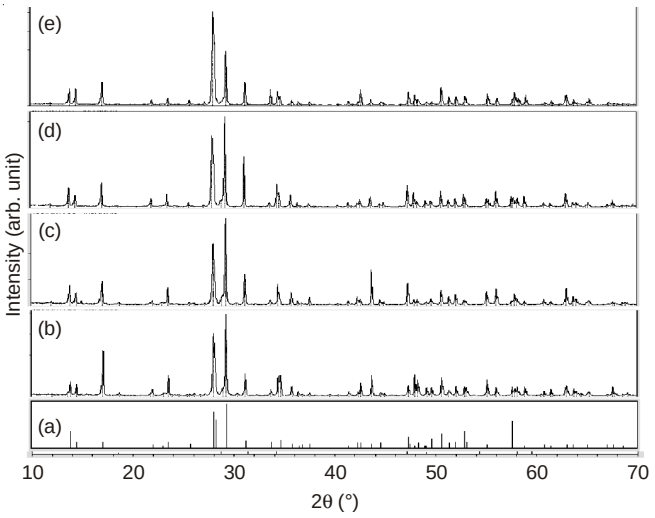

Fig. 1. X-ray diffraction patterns of the (a) JCPDS 45-0472 data of $KY(WO_4)_2$, the synthesized (b) $KY(WO_4)_2$, (c) $KY_{0.8}(WO_4)_2$:$Ho_{0.2}$, (d) $KY_{0.7}(WO_4)_2$:$Ho_{0.1}Yb_{0.2}$, and (e) $KY_{0.5}(WO_4)_2$:$Ho_{0.05}Yb_{0.45}$ particles

Fig. 2 shows a SEM image of the synthesized $KY_{0.5}(WO_4)_2$:$Ho_{0.05}Yb_{0.45}$ particles. The as-synthesized sample is well

crystallized with a fine and homogeneous morphology and particle size of 2-5 μm. It is noted that the structure has a monoclinic-phase after partial substitution of Y^{3+} by Ho^{3+} and Yb^{3+} ions and the ions are effectively doped into crystal lattices of the $KY(WO_4)_2$ phase. The microwave-modified sol-gel process of double tungstates provides the energy to synthesize the bulk of the material uniformly, so that fine particles with controlled morphology can be fabricated in a short time period. The method is a cost-effective way to provide highly homogeneous products and is easy to scale-up, it is a viable alternative for the rapid synthesis of upconversion particles.

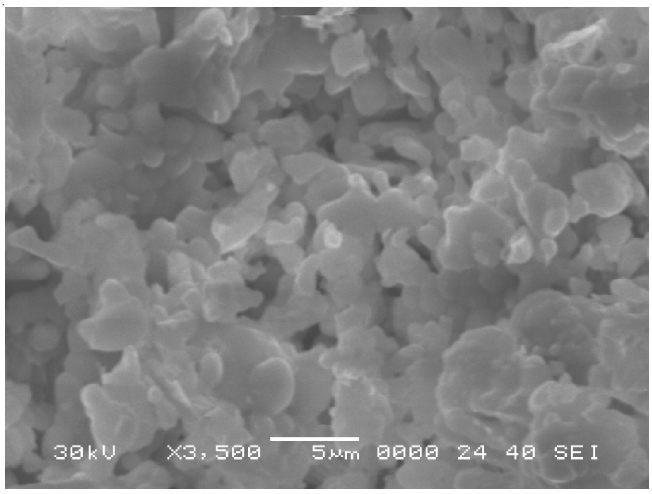

Fig. 2. Scanning electron microscopy image of the synthesized $KY_{0.5}(WO_4)_2$:$Ho_{0.05}Yb_{0.45}$ particles

Fig. 3 shows the upconversion photoluminescence emission spectra of the as-prepared (a) $KY(WO_4)_2$, (b) $KY_{0.8}(WO_4)_2$:$Ho_{0.2}$, (c) $KY_{0.7}(WO_4)_2$:$Ho_{0.1}Yb_{0.2}$ and (d) $KY_{0.5}(WO_4)_2Ho_{0.05}Yb_{0.45}$ particles excited under 980 nm at room temperature. The upconversion intensities of (c) $KY_{0.7}(WO_4)_2$:$Ho_{0.1}Yb_{0.2}$ and (d) $KY_{0.5}(WO_4)_2Ho_{0.05}Yb_{0.45}$ particles exhibited yellow emissions based on a strong 550 nm emission band in the green region and a very strong 655 nm emission band in the red region. The upconversion intensities of (a) $KY(WO_4)_2$ and (b) $KY_{0.8}(WO_4)_2$:$Ho_{0.2}$ particles were not detected. The upconversion intensity of (d) $KY_{0.5}(WO_4)_2Ho_{0.05}Yb_{0.45}$ is much higher than that of (c) $KY_{0.7}(WO_4)_2$:$Ho_{0.1}Yb_{0.2}$ particles. The strong 550 nm emission band in the green region correspond to the $^5S_2$/$^5F_4 \rightarrow {}^5I_8$ transition, while the very strong emission 655 nm band in the red region corresponds to the $^5F_5 \rightarrow {}^5I_8$ transferred to the activator where radiation can be emitted. The Ho^{3+} ion activator is the luminescence center for these upconversion particles and the sensitizer Yb^{3+} enhances effectively the upconversion luminescence intensity because of the efficient energy transfer from Yb^{3+} to Ho^{3+}.

Fig. 4 shows schematic energy level diagrams of Ho^{3+} ions (activator) and Yb^{3+} ions (sensitizer) in the as-prepared $KY_{1-x}(WO_4)_2$:Ho^{3+}/Yb^{3+} samples and the upconversion mechanisms accounting for the green and red emissions during 980 nm laser excitation. The upconversion emissions are generated by a two photon process through excited state absorption (ESA) and energy transfer (ET). Initially, the Yb^{3+} ion sensitizer is excited from the $^2F_{7/2}$ level to the $^4F_{5/2}$ level under excitation of 980 nm pumping and transfers its energy

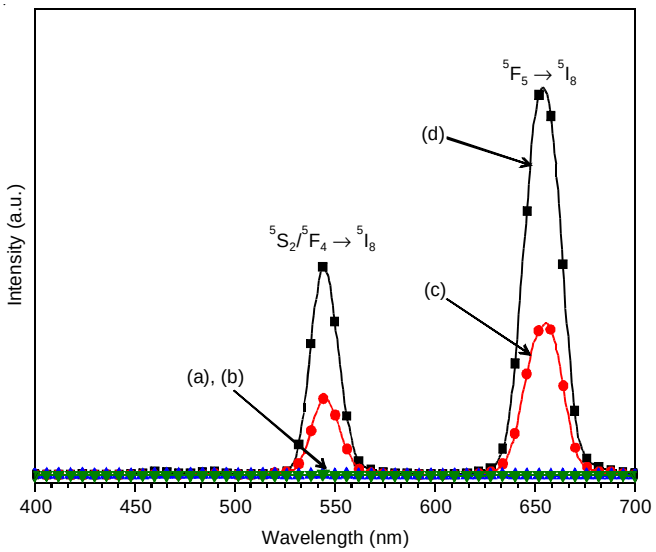

Fig. 3. Upconversion photoluminescence emission spectra of (a) $KY(WO_4)_2$, (b) $KY_{0.8}(WO_4)_2$:$Ho_{0.2}$, (c) $KY_{0.7}(WO_4)_2$:$Ho_{0.1}Yb_{0.2}$ and (d) $KY_{0.5}(WO_4)_2Ho_{0.05}Yb_{0.45}$ particles excited under 980 nm at room temperature

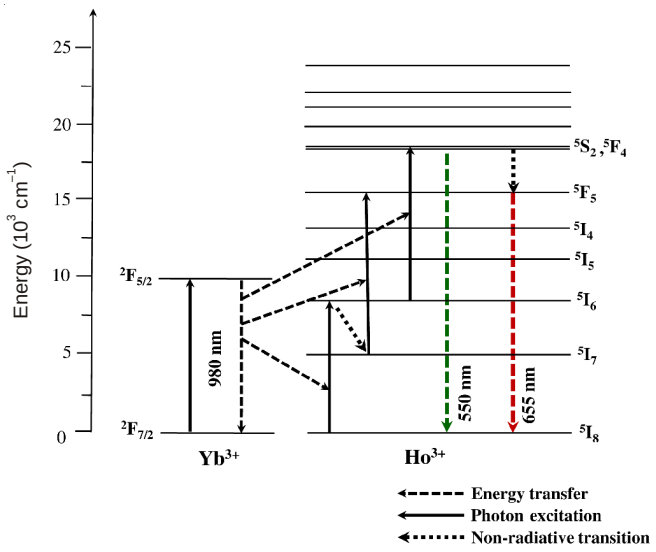

Fig. 4. Schematic energy level diagrams of Ho^{3+} ions (activator) and Yb^{3+} ions (sensitizer) in the as-prepared $KY_{1-x}(WO_4)_2$:Ho^{3+}/Yb^{3+} system and the upconversion mechanisms accounting for the green and red emissions under 980 nm laser excitation

to Ho^{3+} ions. Then Ho^{3+} ions is populated from the $^5I_8$ ground state to $^5I_6$ excited state. This is a phonon-assisted energy transfer process because of energy mismatch between $^2F_{5/2}$ level of Yb^{3+} and $^5I_6$ level of Ho^{3+}. Secondly, the Ho^{3+} in $^5I_6$ level is excited to $^5S_2$ or $^5F_4$ level by the same energy transfer from Yb^{3+}. In addition, the $^5S_2$/$^5F_4$ level of Ho^{3+} can also populated through excited state absorption. Finally, the green emission around 550 nm corresponding to $^5S_2$/$^5F_4 \rightarrow {}^5I_8$ transition takes place. For red emission, the population of the $^5F_5$ level is generated by two different channels. One channel is that Ho^{3+} in the $^5S_2$/$^5F_4$ level relaxes non-radiatively to the $^5F_5$ level. Another channel is closely related to the $^5I_7$ level populated by non-radiative relaxation from the $^5I_6$ excited state. The Ho^{3+} in $^5I_7$ level is excited to the $^5F_5$ level by the energy transfer from Yb^{3+}. Therefore, the red emission around 655 nm is corresponding to the $^5F_5 \rightarrow {}^5I_8$ transition[11,12].

Fig. 5 shows the Raman spectra of the synthesized (a) $KY(WO_4)_2$(KYW), (b) $KY_{0.8}(WO_4)_2$:$Ho_{0.2}$(KYW:Ho), (c) $KY_{0.7}(WO_4)_2$:$Ho_{0.1}Yb_{0.2}$(KYW:HoYb) and (d) $KY_{0.5}(WO_4)_2$:$Ho_{0.05}Yb_{0.45}$ (KYW:HoYb#) particles excited by the 514.5 nm line of an Ar ion laser at 0.5 mW. The internal modes for the (a) $KY(WO_4)_2$(KYW) particles were detected at 350, 378, 442, 530, 686, 765, 810 and 905 cm^{-1}. The well-resolved sharp peaks for the $KY(WO_4)_2$ particles indicate a high crystallinity state of the synthesized particles. The internal vibration mode frequencies are dependent on the lattice parameters and the degree of the partially covalent bond between the cation and molecular ionic group $[WO_4]^{2-}$. The Raman spectra of the (b) $KY_{0.8}(WO_4)_2$:$Ho_{0.2}$(KYW:Ho) and (c) $KY_{0.7}(WO_4)_2$: $Ho_{0.1}Yb_{0.2}$ (KYW:HoYb) and (d) $KY_{0.5}(WO_4)_2$:$Ho_{0.05}Yb_{0.45}$ (KYW:HoYb#) particles indicate the domination of strong peaks at higher frequencies (932, 1050, 1125 and 1250 cm^{-1}) and a weak peak at lower frequency (320 cm^{-1}). The Raman spectra of (b) $KY_{0.8}(WO_4)_2$:$Ho_{0.2}$ (KYW:Ho), (c) $KY_{0.7}(WO_4)_2$: $Ho_{0.1}Yb_{0.2}$(KYW: HoYb) and (d) $KY_{0.5}(WO_4)_2$:$Ho_{0.05}Yb_{0.45}$ (KYW:HoYb#) particles prove that the doping ions can influence the structure of the host materials. The combination of a heavy metal cation and the large inter-ionic distance for Ho^{3+} and Yb^{3+} substitutions in La^{3+} sites in the lattice result in a low probability of upconversion and phonon-splitting relaxation in $KY_{1-x}(WO_4)_2$ crystals. It may be that these strong and strange effects are generated by the disorder of the $[WO_4]^{2-}$ groups with the incorporation of the Ho^{3+} and Yb^{3+} elements into the crystal lattice or by a new phase formation.

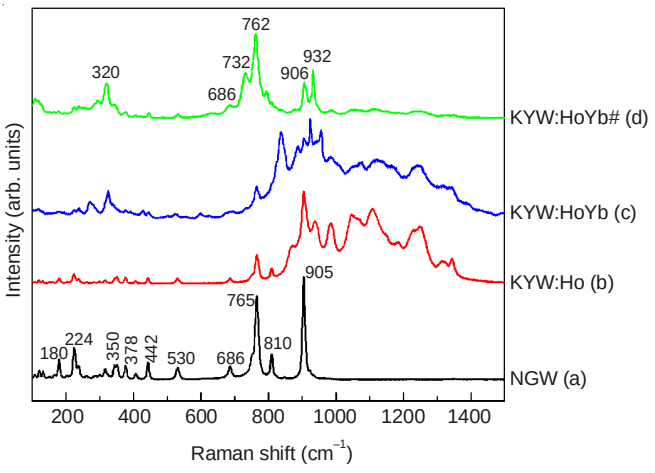

Fig. 5. Raman spectra of the synthesized (a) $KY(WO_4)_2$(KYW), (b) $KY_{0.8}(WO_4)_2$:$Ho_{0.2}$ (KYW:Ho), (c) $KY_{0.7}(WO_4)_2$:$Ho_{0.1}Yb_{0.2}$(KYW:HoYb) and (d) $KY_{0.5}(WO_4)_2$:$Ho_{0.05}Yb_{0.45}$ (KYW:HoYb#) particles excited by the 514.5 nm line of an Ar ion laser at 0.5 mW

Conclusion

The double tungstate $KY_{1-x}(WO_4)_2$:Ho^{3+}/Yb^{3+} yellow phosphors with doping concentrations of Ho^{3+} and Yb^{3+} (x = Ho^{3+} + Yb^{3+}, Ho^{3+} = 0.05, 0.1, 0.2 and Yb^{3+} = 0.2, 0.45) were successfully prepared by the microwave-assisted sol-gel method. Well-crystallized particles formed after heat-treatment at 900 °C for 16 h showed a fine and homogeneous morphology with particle sizes of 2-5 μm. Under excitation at 980 nm, the upconversion intensities of $KY_{0.7}(WO_4)_2$:$Ho_{0.1}Yb_{0.2}$ and $KY_{0.5}(WO_4)_2Ho_{0.05}Yb_{0.45}$ particles exhibited yellow emissions based on a strong 550 nm emission band in the green region and a very strong 655 nm emission band in the red region, which were assigned to the $^5S_2/^5F_4 \rightarrow {}^5I_8$ and $^5F_5 \rightarrow {}^5I_8$ transitions, respectively. The upconversion intensity of $KY_{0.5}(WO_4)_2Ho_{0.05}Yb_{0.45}$ particles was much higher than that of the $KY_{0.7}(WO_4)_2$:$Ho_{0.1}Yb_{0.2}$ particles. The Raman spectra of the $KY_{0.8}(WO_4)_2$:$Ho_{0.2}$, $KY_{0.7}(WO_4)_2$:$Ho_{0.1}Yb_{0.2}$ and $KY_{0.5}(WO_4)_2$:$Ho_{0.05}Yb_{0.45}$ particles indicated the domination of strong peaks at higher frequencies (932, 1050, 1125 and 1250 cm^{-1}) and a weak peak at lower frequency (320 cm^{-1}) induced by the disorder of the $[WO_4]^{2-}$ groups with the incorporation of the Ho^{3+} and Yb^{3+} elements into the crystal lattice or by a new phase formation.

ACKNOWLEDGEMENTS

This study was supported by the Basic Science Research Program through the National Research Foundation of Korea (NRF) funded by Ministry of Science, ICT & Future Planning (2014-046024).

REFERENCES

1. Y.J. Chen, H.M. Zhu, Y.F. Lin, X.H. Gong, Z.D. Luo and Y.D. Huang, *Opt. Mater.*, **35**, 1422 (2013).
2. M. Wang, G. Abbineni, A. Clevenger, C. Mao and S. Xu, *Nanomedicine*, **7**, 710 (2011).
3. M. Lin, Y. Zhao, S.Q. Wang, M. Liu, Z.F. Duan, Y.M. Chen, F. Li, F. Xu and T.J. Lu, *Biotechnol. Adv*, **30**, 1551 (2012).
4. L. Li, W. Zi, H. Yu, S. Gan, G. Ji, H. Zou and X. Xu, *J. Lumin.*, **143**, 14 (2013).
5. C. Ming, F. Song and L. Yan, *Opt. Commun.*, **286**, 217 (2013).
6. N. Xue, X. Fan, Z. Wang and M. Wang, *J. Phys. Chem. Solids*, **69**, 1891 (2008).
7. Z. Shan, D. Chen, Y. Yu, P. Huang, F. Weng, H. Lin and Y. Wang, *Mater. Res. Bull.*, **45**, 1017 (2010).
8. W. Liu, J. Sun, X. Li, J. Zhang, Y. Tian, S. Fu, H. Zhong, T. Liu, L. Cheng, H. Zhong, H. Xia, B. Dong, R. Hua, X. Zhang and B. Chen, *Opt. Mater.*, **35**, 1487 (2013).
9. W. Xu, H. Zhao, Y. Li, L. Zheng, Z. Zhang and W. Cao, *Sens. Actuators B*, **188**, 1096 (2013).
10. C.S. Lim, *Mater. Res. Bull.*, **47**, 4220 (2012).
11. Y. Xu, Y. Wang, L. Shi, L. Xing and X. Tan, *Opt. Laser Technol.*, **54**, 50 (2013).
12. X. Li, Q. Nie, S. Dai, T. Xu, L. Lu and X. Zhang, *J. Alloys Comp.*, **454**, 510 (2008).